Unexpected thermo-elastic effects in liquid glycerol by mechanical deformation

Eni Kume, Alessio Zaccone, Laurence Noirez

Physics of Fluids

Unexpected thermo-elastic effects in liquid glycerol by mechanical deformation

Cite as: Phys. Fluids **33**, 072007 (2021); https://doi.org/10.1063/5.0051587
Submitted: 26 March 2021 . Accepted: 26 May 2021 . Published Online: 09 July 2021

Eni Kume, Alessio Zaccone, and Laurence Noirez

Physics of Fluids ARTICLE scitation.org/journal/phf

Unexpected thermo-elastic effects in liquid glycerol by mechanical deformation

Cite as: Phys. Fluids 33, 072007 (2021); doi: 10.1063/5.0051587
Submitted: 26 March 2021 · Accepted: 26 May 2021 ·
Published Online: 9 July 2021 · Publisher error corrected: 12 July 2021

Eni Kume,[1] Alessio Zaccone,[2,3] and Laurence Noirez[1,a)]

AFFILIATIONS

[1]Laboratoire Léon Brillouin (CEA-CNRS), Univ. Paris-Saclay, 91191 Gif-sur-Yvette Cedex, France
[2]Department of Physics "A. Pontremoli", University of Milan, 20133 Milan, Italy
[3]Department of Chemical Engineering and Biotechnology, University of Cambridge, Philippa Fawcett Drive, CB30AS Cambridge, United Kingdom and Cavendish Laboratory, University of Cambridge, JJ Thomson Avenue, CB30HE Cambridge, United Kingdom

[a)]Author to whom correspondence should be addressed: Laurence.noirez@cea.fr

ABSTRACT

It is commonly accepted that shear waves do not propagate in a liquid medium. The shear wave energy is supposed to dissipate nearly instantaneously. This statement originates from the difficulty to access "static" shear stress in macroscopic liquids. In this paper, we take a different approach. We focus on the stability of the thermal equilibrium while the liquid (glycerol) is submitted to a sudden shear strain at sub-millimeter scale. The thermal response of the deformed liquid is unveiled. The liquid exhibits simultaneous and opposite bands up to about $+0.04$ to $-0.04\,^{\circ}$C temperature variation, while keeping the global thermal balance unchanged. The sudden thermal changes and the long thermal relaxation highlight the ability of the liquid to convert the step strain energy in non-uniform thermodynamic states. The thermal effects depend nearly linearly on the amplitude of the deformation supporting the hypothesis of a shear wave propagation (elastic correlations) extending up to several hundreds micrometers. This new physical effect can be explained in terms of the underlying phonon physics of confined liquids, which unveils a hidden solid-like response with many similarities to glassy systems.

I. INTRODUCTION

Mechanical studies focus on the response of a sample to external forces and deformations. In stress relaxation measurements, the sample is submitted to nearly instant deformation either in elongation or in shear geometry. The stress relaxation is used to understand the underlying mechanisms of different materials to an external mechanical field. This traditional stress relaxation protocol is applied to solids or viscoelastic solid materials, such as metals, glassy polymers,[1,2] or liquid crystals,[3] with remarkable similitudes. However, for liquids, their short molecular relaxation times (e.g., $\tau_{Glycerol} = 10^{-9}$ s)[4,5] are expected to dissipate nearly instantly shear stress for excitations lower than MHz or GHz, making mechanically induced stress relaxation studies hypothetically irrelevant.

This paper challenges the above assertion; we experimentally prove that liquids (glycerol) exhibit a thermal response, at room temperature and atmospheric pressure, to a constant mechanical shear strain by applying a step strain function at the sub-millimeter (100—250 μm) scale and model it using the Anderson-Grüneisen relation. In contrast to conventional stress relaxation measurements that are believed to be irrelevant for molecular liquids, highlighting a stress-induced thermal response proves that liquids can store shear energy at the mesoscopic scale.

The thermal radiation is a probe of the local dynamics (rotational and vibrational motions of molecules). At room temperature, the black body thermal radiation emits in the MWIR (Mid-Wave InfraRed band between 3 and 5.5 μm) and LWIR (Long Wave InfraRed band between 7 and 14 μm). The infrared signature reveals the temperature using well established laws: the blackbody Planck law. We evidence the emergence of hot and cold non-uniform temperature bands in the liquid glycerol upon applying a step strain field. These strain-induced thermodynamic regions are the non-ambiguous proof that the shear energy can be thermally stored in the liquid, relaxes slowly leading to new solutions of its total free energy.

II. METHODS

Glycerol (99% purity) was used for the measurements at room temperature ($\sim$22 °C), far away from any critical point (e.g., for glass transition, $T_g = -93\,^{\circ}$C). The glycerol is a much studied liquid due its

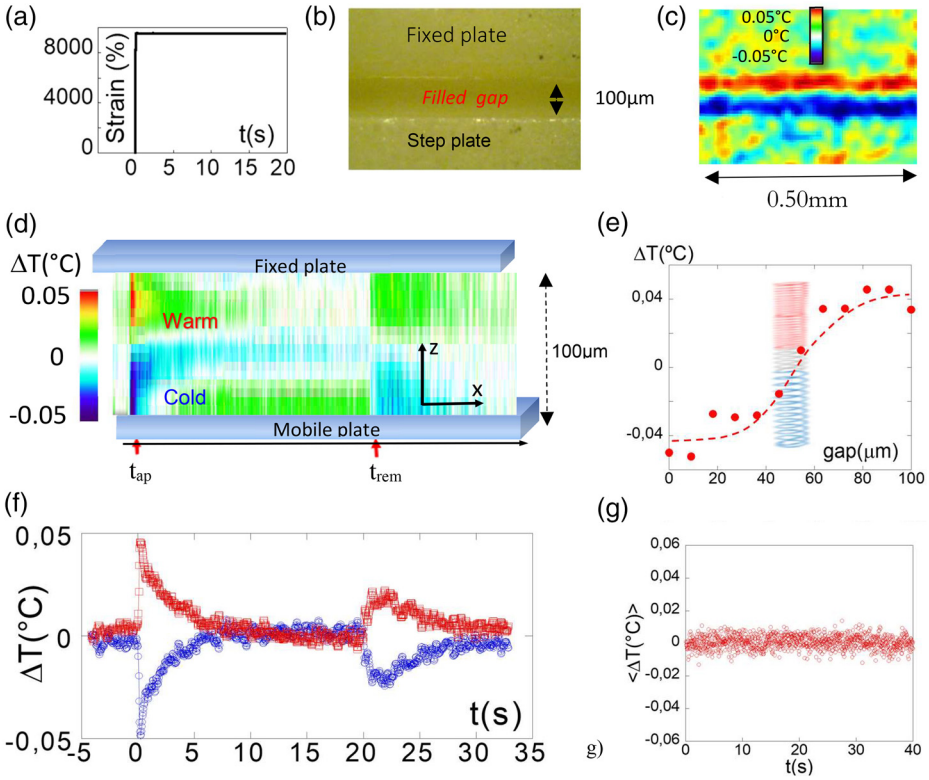

FIG. 1. (a) Step strain function (real data—forward step $\gamma = 9500\%$). (b) Optical photograph of the plates and the gap. (c) Corresponding thermal snapshot recorded at the early times of the relaxation process (room temperature, $\gamma = 4000\%$, $t = t_0 + 0.25$ s); hot and cold thermal zones (about 40 μm wide) are observed in the liquid while surfaces are immobile. The pixel resolution is 2.5 μm. (d) Real-time thermal mapping of the liquid temperature after a step strain mechanical stimulus at t_{ap} (forward motion, $\gamma = 9500\%$) followed by a slower backward step ($\gamma = -9500\%$) to the initial position at t_{rem} ($t_{rem} - t_{ap} = 20$ s) (room temperature measurements). Forward and backward steps were achieved in 0.03 s and 0.08 s, respectively, by displacing the bottom plate. The x axis is the time; the z axis is along the gap thickness (100 μm). The color index indicates the temperature variation with respect to the equilibrium temperature (at $t < t_{ap}$). (e) Temperature variation profile along the gap (z-axis) at $t = t_{ap} + \Delta t$, averaged over three successive frames ($t_{tot} = 0.11$ s) just after t_{ap}. The continuous red line is an eye-guide to outline the continuous variation of the temperatures through the gap. The cartoon illustrates a spring to image the compressed/dilated zones through the gap. (f) Thermal bands corresponding to Fig. 1(d) (3 pixels width): Top (hot) band: (red square) □ and bottom (cold) band: (blue circle) ○. (g) Temperature variation integrated over the whole gap vs time during the experiment (data of Fig. 1).

extremely wide range of uses and biocompatibility. This glass former exhibits at room temperature with a viscosity about a hundred times higher than liquid water ($\eta_{glycerol} = 1.41$ Pa·s).

The liquid is set in the gap between α-alumina surfaces to ensure a high wetting of the liquid on the fixture [plate–plate disks of 40 mm of diameter—Fig. 1(b)]. The gap thickness varies from 100–250 μm. The shear strain is defined as $\gamma = \delta l/e$, where δl is the displacement and e is the gap thickness. The deformation (step strain) is a (nearly) Heaviside function of time $H(t)$, where $H(t) = \begin{cases} 0, & t_{ap} < 0 \\ \gamma, & t_{ap} > 0 \end{cases}$ [Fig. 1(a)]. The step lasts 0.03 s, and the strain value ranges from 20% to 9500%, depending on the gap thickness [using a shear strain-controlled rheometer (TA-ARESII)]. The system (plates and confined liquid) was left at rest for more than an hour before the start of the experiment. A time delay of 5–10 min was enforced between two successive step strains to ensure the thermal equilibrium of the sample and with the environment. The only energy provided to the liquid is, thus, the work generated by the displacement of the moving plate.

A micro-bolometric detector array of 382 × 288 pixels embedded in a camera using a relay lenses with a focal length of 7.5 mm and a numerical aperture F/1 detects the radiation emitted by the liquid in the near-infrared range. The infrared focal plane array is set on the liquid surface with the lenses 15 mm away from the edge of the plate–liquid–plate, ensuring non-contact measurements (Scheme 1). The depth of the thermal field is estimated at 0.85 mm for glycerol. The two-dimensional thermal images were captured at the frame rate of 27 Hz. The images were corrected by subtraction of the equilibrium median value.

III. RESULTS

Figure 1 describes real-time thermal radiation emitted at room temperature by glycerol submitted to a step (shear) strain deformation ($t \geq t_{ap}$). Prior to each measurement, the liquid is in a stable thermal equilibrium state for a long time (>5–10 min) [Fig. 1(d) at $t < t_{ap}$]. At t_{ap}, an instant variation of temperature is observed. Two bands of opposite temperature are immediately created along the strain direction disrupting the initial temperature stability [Fig. 1(c)]. The sudden

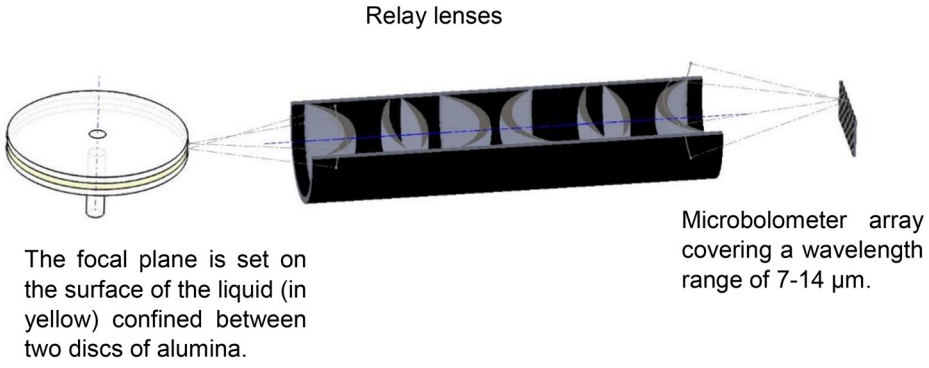

SCHEME 1. Illustration of the infrared-relay lens setup used to magnify the thermal image of the several hundred micrometers liquid gap.

splitting of the liquid in two regions of opposite temperature variation is followed by a slow thermal relaxation. The highest temperature variations ($|\Delta T| = 0.04 \pm 0.01\,^{\circ}C$) are reached at the onset of the relaxation at the highest step strain (9500%) [Fig. 1(e)] and are located at mid-distance between the middle of the gap and the surface with the cold band next to the plate at the origin of the shear strain. At t_{rem} [Fig. 1(e)], the applied shear strain is removed by moving the surface back to its initial equilibrium position ("backward" displacement). The backward step generates a new thermal response pointing out a reversible thermal effect (the smaller thermal amplitude is attributed to a longer ramp for the backward step: 0.08 against 0.03 s for the forward displacement—the ramps are imposed by the software). We now focus on the first part of the thermal liquid response ($t_{ap} < t < t_{rem}$). Figure 1(f) shows the profile of the temperature variation across the gap at the early instants of the step strain. The smooth temperature profile indicates that the hot and the cold bands are not independent regions but two sides of the same thermal effect. The middle of the gap corresponds to the temperature at rest (equilibrium temperature).

Though the thermal study reveals that significant temperature changes occur during relaxation [forward and (slow) backward], the overall average liquid temperature is unchanged [Fig. 1(g)]; the mean gap value over the whole relaxation process is $\overline{\Delta T} \approx -2 \times 10^{-4}\,^{\circ}C$ with a standard deviation of 4×10^{-3}. It means that the global volume is kept constant during the whole relaxation process. Consequently, the temperature variations correspond to local non-equilibrium pressure variations that compensate each other. No energy transfer took place between the liquid and the environment during the relaxation. Also the energy stored during the 0.03 s strain step did not generate viscous heating [also in agreement with a Nahme number (also known as Brinkman number) lower than 1 (here $Na = 0.041$ at $\gamma = 9500\%$), where $Na = \eta_0 \beta e^2 \dot{\gamma}^2/\kappa$, with η_0 being the viscosity, $\beta = -(1/\eta_0)(d\eta/dT)$, e the gap thickness , $\dot{\gamma}$ the shear rate, and κ the thermal conductivity].

Figure 2(a) details the evolution and the modeling of the thermal profile of the hot band (symmetrical evolution is observed for the cold one). The time to reach the maximum temperature variation is 0.19 s [Fig. 2(a)]. The time of the ramp of the step strain (time needed for the strain to establish) is 0.03 s; as a result, during the estimated time of 0.16 s, the liquid stores the shear energy as potential (internal) energy in the liquid. This potential energy manifests as changes of macroscopic properties, such as the temperature. The duration of the ramp is the same regardless of the strain value, thus increasing the strain in each measurement is equivalent to increasing the shear rate (energy rate transferred to the liquid).

The inset in Fig. 2(a) focuses on the early times of the thermal response of the hot band, during the step strain (red circles). The temperature increases rapidly as the step strain is applied (left of dotted line), and then it decreases rapidly with an overshoot, followed by a small oscillation (second overshoot). The short time thermal response can be described by a second order transfer function $H_{nf}(s) = H_0[{\omega_0}^2/(s^2 + 2\zeta\omega_0 s + {\omega_0}^2)]$, where ω_0 is the natural frequency, ζ is the damping ratio, s the Laplace variable, and H_0 the system gain. The mathematical solution is written as[6]

$$\Delta T_{fit}(t) = A\left[1 - \frac{e^{-\zeta\omega_n t}}{\sqrt{1-\zeta^2}}\cos\left(\omega_n\sqrt{1-\zeta^2}\,t - \varphi\right)\right], \quad (1)$$

where A is a constant, φ is a phase shift, and ΔT_{fit} is the temperature variation based on the second order step response. Equation (1) is fitted to the initial thermal response (Fig. 2, inset). From the fitting of Eq. (1), we obtain $\zeta = 0.35 \pm 0.02$, while $\omega_n = 8 \pm 0.3$ rad/s. It shows that the order of the natural frequency ω_n is of the order of Hz; i.e., it describes a collective thermal effect. The characteristic overshoot is noticeable at 0.3 s [Fig. 2(a) inset], as expected for the underdamped case ($\zeta < 1$).[6] The steady state value (asymptotic value at long timescale) is derived from the overshoot value with the equation:[7]

$$\frac{(\text{Overshoot value-Steady state value})}{\text{Steady state value}} = \exp\left(-\frac{-\zeta\pi}{\sqrt{1-\zeta^2}}\right). \quad (2)$$

Equation (2) foresees an asymptotic value $\Delta T_{t\to\infty} = 0.03\,^{\circ}C$. Fig. 2(a) shows that the thermal relaxation does not reach this value but returns to equilibrium.

The long-time thermal relaxation to equilibrium (both cold and hot bands relax symmetrically) can be modeled by a stretched exponential decay,

$$\Delta T(e,\gamma) = \Delta T_{max}(e^{-t/\tau})^{\beta} \quad (3)$$

[Fig. 2(a), right of the dotted line], with the exponent estimated at $\beta \approx 0.8$–0.85 and a relaxation time τ dependent on the gap thickness and the strain value [Fig. 2(b)]. The relaxation time τ decreases by increasing the gap ruling out an interpretation in terms of molecular times ($\tau \approx 2$–5.5 s for 100 μm, $\tau \approx 0.5$–1.8 s for $150 < e < 200$ μm,

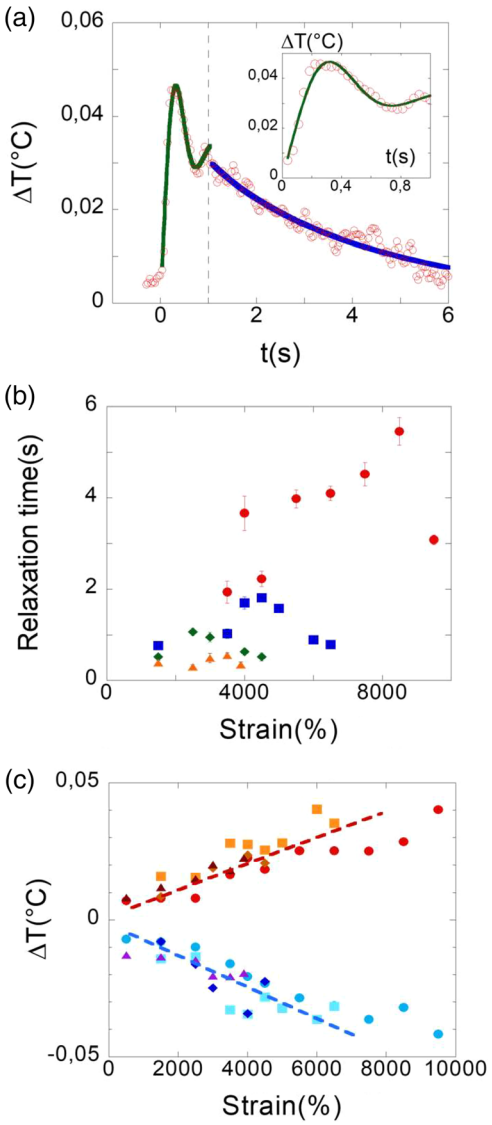

FIG. 2. (a) Modeling of the thermal response of the hot band of glycerol illustrated at 0.100 mm, 9500%. Green and blue lines represent the fits with Eqs. (1) and (3), respectively. Inset: detail and fit of the early times (left of the dotted line) of the thermal overshoot (green line). (b) Relaxation time τ (s) of the top (hot) thermal band vs shear strain amplitude (after a 0.03 s strain step) at different gap thicknesses: 100 (red bullet), 150 (dark blue square), 200 (green diamond), and 250 μm (yellow triangle). (c) Amplitude of the temperature variation vs strain at different gap thicknesses. Warm band: 100: (red bullet), 150: (orange square), 200: (brown diamond), and 250 μm: (brown triangle). Cold band: 100: (blue bullet), 150: (sky blue square), 200: (dark blue diamond), and 250 μm: (magenta triangle). Room temperature measurements.

and $\tau \approx 0.3$–0.5 s for 250 μm). An interpretation in terms of thermal diffusion between hot and cold bands can be ruled out. The thermal diffusion time can be calculated using $\tau_{diff} = h^2/D$, with h being the width of the hot band and D the thermal diffusivity.[8] The value $\tau_{diff} = 0.016$ s excludes the thermal diffusion as a relevant mechanism.

Hence, we have seen that the temperature profiles behave asymptotically like

$$\Delta T(t) \sim \exp(-\zeta\omega_n t) = \exp(-t/\tau), \tag{4}$$

where ω_n is a normal mode (eigenfrequency) of the system. The second equality defines a characteristic relaxation time $\tau = (\zeta\omega_n)^{-1}$. According to this definition, the increase in τ upon decreasing the thickness e could be explained with the decrease in damping ζ upon decreasing e; i.e., an increase in rigidity in agreement with the observed increase in shear elasticity at small scales.[9–14]

It is well known that stretched exponential relaxation arises when there is a distribution of relaxation times in the system (e.g., from dynamical heterogeneity which is ubiquitous in glassy systems),

$$\exp(-t/\tau)^{\beta} \approx \int_0^{\infty} \rho(\tau)\exp(-t/\tau)d\tau, \tag{5}$$

where $\rho(\tau)$ is a suitable distribution of relaxation times, which must satisfy few mathematical requirements.[15] As τ in our system is related to the normal mode ω_n of the liquid system, the distribution $\rho(\tau)$ must be given by the distribution of vibrational normal modes in the liquid, $\rho(\omega_n)$, also known in condensed matter physics as the vibrational density of states (VDOSs). Hence, upon using the VDOS of a glassy liquid in Eq. (5), we obtain[16–18]

$$\Delta T(t) \sim \exp(-t/\tau)^{\beta} \approx \int_0^{\infty} \rho(\omega_n)\exp(-\zeta\omega_n t)d\omega_n, \tag{6}$$

with $\tau = (\zeta\omega_n)^{-1}$. The validity of Eq. (6) for the case of glycerol in the supercooled liquid state was numerically verified in Ref. 15. It was shown that the boson peak (excess of vibrational modes over the Debye level $\sim \omega_n^2$) in the VDOS represents a crucial requirement for Eq. (6) to produce a stretched-exponential relaxation in the measured dielectric response of glycerol. Therefore, the experimentally observed stretched-exponential profile in the current system may suggest the existence of low-energy transverse phonon modes of the kind that constitute the boson peak excess of low-energy modes in glasses. In turn, this directly hints to the existence of long-range shear elastic waves in the sub-millimeter confined glycerol.

This picture based on the existence of underlying low-frequency shear modes akin to transverse phonons (the existence of which has been demonstrated also for simple liquids[17–20]) may also explain the emergence of the cold and the hot bands following the shear strain deformation. The cold band is associated with regions where the fluid is locally expanded, whereas the hot band is associated with regions where the fluid is locally compressed. These regions are macroscopically large since they contain a huge number of molecules; accordingly, it makes sense to define long-wavelength phonon modes that live in these regions. In the hot/compressed regions, the volume V of the region gets reduced, whereas in the cold/expanded regions, the volume V is enlarged. Let us recall the definition of the Grüneisen parameter, $\gamma = -\frac{d\ln\omega_n}{d\ln V}$.

As the Grüneisen parameter γ is normally positive for liquids,[21] this relation gives (upon integration) that the phonon frequency ω_n increases as the volume V decreases, whereas ω_n decreases as the volume V increases. Since the vibrational frequency is related to temperature, via $T = h\omega_n/k_B$, it is clear that T increases in the regions where V decreases ("compressed" regions), whereas T decreases in the

regions where V increases ("expanded" regions), thus leading to a hot and a cold band for the compressed and the expanded regions, respectively. The same result can be obtained by using the Anderson-Grüneisen relation,[22]

$$\gamma = -\frac{d\ln T}{d\ln V},$$

which more directly leads to the same result and applies for isentropic processes, hence, also for adiabatic processes; in our case, the entropy production is, indeed, small as the average temperature does not change appreciably [Fig. 1(g)].

Figure 2(c) shows the influence of the strain amplitude on the temperature variation in the hot and the cool parts. The evolution is symmetrical (positive and negative temperature variations) and approximately of the same magnitude for each strain value. The amplitude of the temperature variation increases nearly linearly with increasing strain [Fig. 2(c)]. The strain dependence is little influenced by the thickness for the tested gap (within 100–250 μm) indicating that the thermal variation is mainly a bulk property. The nearly linear strain-dependence of the thermal amplitude defines negative and positive thermo-mechanical constants. The constants $\lambda = (\Delta T/T)/\gamma$ are about $\lambda_{shear} \sim -0.15 \times 10^{-4}$ for the cold band and $\lambda_{shear} \sim +0.12 \times 10^{-4}$ for the hot band at T = 300 K. These values indicate relative variation of temperature per stretching unit. The thermo-elastic constant of steel sheets is typically about $\lambda_{elongational} = (\Delta T/T)/E \cong 0.45$, where E is the elongational strain.[23] The temperature variation is much higher in solids and is always positive consistent with dissipative processes (moving defects). The liquid thermomechanical constants are about three decades lower indicating a much weaker energy mechanism that might be compatible with Van der Waals interactions.[10–14]

The study of the thermal profiles at various strain values and gap thicknesses (within 100–250 μm) holds a response similar to that in Fig. 1(d). The liquid splits in two thermal bands; i.e., the cold part being close to the plate which moved and the hot part being close to the fixed surface. This observation might be understood as a liquid "stretching" or expansion initiated by the moving plate and, thus, the temperature drop as described by the Grüneisen relation. The condition of constant total volume, in turn, implies the generation of the hot band in the compressed region of the liquid volume.

At a larger gap thickness, we observe the creation of multiple and alternated hot and cold bands that seem to be characterized by a limited width of about 80–100 μm. (Figure 3 illustrates the multiple thermal bands at 500 μm.) We associate the bandwidth to the limit of propagation of the shear wave. As mentioned in Refs. 18, 19, and 24–28, the propagation length of shear waves in a liquid medium is finite—a phenomenon known as the k-gap.[19,24,28] In practice, shear waves are expected to vanish on length scales larger than $\sim 1/k_g$, where k_g represents the wavevector above which elastic shear waves can propagate. For glycerol, we estimate that $1/k_g$ is on the order of 1–2 μm, hence, smaller than the liquid gap. This implies that multiple bands can occur for large thickness values, and each band corresponds to a region where locally elastic shear waves can propagate.

The above results demonstrate unexpected thermo-elastic effects in liquids, which can be explained in terms of the unsuspected ability of liquids to support low-frequency shear waves. The experiments show that, upon a shear step deformation of large amplitude and at mesoscopic scale, a viscous liquid (glycerol) changes its

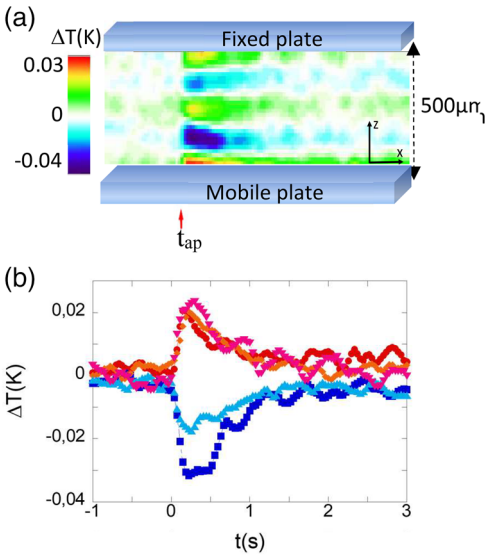

FIG. 3. (a) Thermal mapping of liquid glycerol at a large gap (500 μm) upon shear step strain $\gamma = 1500\%$ (maximum available displacement) applied at t_{ap}. The shear step was achieved in 0.03 s by moving the bottom plate. The x axis is the time; the z axis is along the gap thickness. The color index indicates the temperature variation with respect to the equilibrium temperature (at $t < t_{ap}$). (b) Thermal profiles corresponding to (a). Bottom (closest to moving plate) band: blue square, intermediate between bottom and middle regions band: brown bullet, middle band: red diamond, intermediate between top and middle regions band: sky blue triangle, and top band: pink iverted triangle.

thermodynamic state. The liquid loses its temperature homogeneity creating two major thermodynamic regions, where the temperature deviates symmetrically from the equilibrium one. These mechanically induced thermodynamic rearrangements imply an ability of the liquid to store the strain energy in its normal modes. Hot and cold thermal bands indicate that the liquid does not relax immediately: some of the shear energy is stored in the liquid, leading to the creation of local thermal bands. The thermal variations of the bands are of opposite values, leading to an average thermal compensation and a global thermal invariance (adiabaticity). The early time thermal response [Fig. 2(a) inset], described by a second-order response, means, indeed, that there is an exchange of energy between two storages. One is the external shear strain, and the others are viscous and elastic elements in the liquid. Equivalent systems are damped mechanical oscillators like electronic RLC circuit,[7] hydro-mechanical or spring-mass-damper systems. After the overshoot, the liquid loses the gain from the step shear strain, though constant strain is maintained. This long-time thermal relaxation shows a stretched exponential nature, similar to the dielectric α relaxation of glycerol near glass transition,[17] elucidating a solid-like behavior of the confined liquid glycerol. However, the timescale of the thermal relaxations is neither related to a slow relaxation heat transfer process nor to short molecular relaxation times. As the phenomenon is fast without heat transfer, the observed thermal effects (negative and positive temperature variations) are related to internal energy changes (adiabatic processes) that minimize the system free energy. This can be explained in terms of the local dilation/compression leading to local cooling/heating as a consequence of the

relationship between temperature variation and volume variation established by the Grüneisen or Anderson-Grüneisen relation. In turn, the shear waves behave like phonons in solids and provide an explanation for the observed thermal bands (hot and cold in compressed and dilated regions, respectively) in terms of the Grüneisen parameter relation, which is well known for phonons in solids, and relates local temperature variations to local volume variations as observed in the experiments (since phonons are standing waves in the local density field). The formation and relaxation of thermal bands, and the invariance of the global temperature are the proof that elastic shear waves propagate in liquids at the scale of hundreds of micrometers. An elastic-like process achieved nearly without heat transfer is characteristic of adiabatic shear elasticity. The ability of liquids to support shear waves was already experimentally uncovered,[8–13,22,24] and theoretically suggested.[19,20,24–28]

These results suggest that the thermo-elastic response of liquids should be more systematically considered in order to achieve a deeper understanding of the liquid state. With confined liquid systems gaining more and more relevance, from the micro- (e.g., microfluidics) to even the nano scale (e.g., nanofluidics),[29] this effect may play a prominent role for the manipulation of liquids at the smallest scales in future research.

ACKNOWLEDGMENTS

We thank P. Baroni for instrumental innovation and assistance. This work has received funding from the European Union's Horizon 2020 Research and Innovation Programme under the Marie Sklodowska-Curie Grant Agreement No. 766007 and LabeX Palm (No. ANR-11-Idex-0003-02).

DATA AVAILABILITY

The data that support the findings of this study are available from the corresponding author upon reasonable request.

REFERENCES

[1]S. Blonski, W. Brostow, and J. Kuba't, "Molecular-dynamics simulations of stress relaxation in metals and polymers," Phys. Rev. B **49**, 6494 (1994).
[2]D. W. Van Krevelen, Revised by and K. Te Nijenhuis, "Mechanical Properties of Solid Polymers," in *Properties of Polymers Their Correlation with Chemical Structure, Their Numerical Estimation and Prediction from Additive Group Contributions*, 4th ed. (Elsevier Science, 2009), Chap. 13, p. 383–503.
[3]R. Bartolino and G. Durand, "Plasticity in a smectic a liquid crystal," Phys. Rev. Lett. **39**, 1346 (1977).
[4]L. Comez, D. Fioretto, F. Scarponi, and G. Monaco, "Density fluctuations in the intermediate glass-former glycerol: A Brillouin light scattering study," J. Chem. Phys. **119**, 6032 (2003).
[5]F. Scarponi, L. Comez, D. Fioretto, and L. Palmieri, "Brillouin light scattering from transverse and longitudinal acoustic waves in glycerol," Phys. Rev. B **70**, 054203 (2004).
[6]M. T. Thompson, "Review of signal processing basics," in *Intuitive Analog Circuit Design* (Elsevier, 2014), Chap. 2.
[7]W. Bolton, *Control Systems* (Elsevier, 2002).
[8]J. A. Balderas-López, A. Mandelis, and J. A. García, "Measurements of the thermal diffusivity of liquids with a thermal-wave resonator cavity," Anal. Sci. **17**, s519 (2001).
[9]B. V. Derjaguin, U. B. Bazaron, K. T. Zandanova, and O. R. Budaev, "The complex shear modulus of polymeric and small-molecule liquids," Polymer **30**(1), 97 (1989).
[10]L. Noirez, H. Mendil-Jakani, and P. Baroni, "Identification of finite shear-elasticity in the liquid state of molecular and polymeric glass-formers," Philos. Mag. **91**, 1977–1986 (2011).
[11]L. Noirez and P. Baroni, "Revealing the solid-like nature of glycerol at ambient temperature," J. Mol. Struct. **972**, 16–21 (2010).
[12]L. Noirez and P. Baroni, "Identification of a low-frequency elastic behaviour in liquid water," J. Phys.: Condens. Matter **24**(37), 372101 (2012).
[13]P. Lv, Z. Yang, Z. Hua, M. Li, M. Lin, and Z. Dong, "Viscosity of water and hydrocarbon changes with micro-crevice Thickness," Colloids Surf., A **504**, 287 (2016).
[14]Y. Chushkin, C. Caronna, and A. Madsen, "Low-frequency elastic behavior of a supercooled liquid," Europhys. Lett. **83**, 36001 (2008).
[15]D. C. Johnston, "Stretched exponential relaxation arising from a continuous sum of exponential decays," Phys. Rev. B **74**, 184430 (2006).
[16]B. Cui, R. Milkus, and A. Zaccone, "Direct link between boson-peak modes and dielectric α-relaxation in glasses," Phys. Rev. E **95**, 022603 (2017).
[17]B. Cui, R. Milkus, and A. Zaccone, "The relation between stretched-exponential relaxation and the vibrational density of states in glassy disordered systems," Phys. Lett. A **381**, 446–451 (2017).
[18]A. Zaccone, "Relaxation and vibrational properties in metal alloys and other disordered systems," J. Phys.: Condens. Matter **32**, 203001 (2020).
[19]C. Yang, M. T. Dove, V. V. Brazhkin, and K. Trachenko, "Emergence and evolution of the k gap in spectra of liquid and supercritical states," Phys. Rev. Lett. **118**, 215502 (2017).
[20]A. Zaccone and K. Trachenko, "Explaining the low-frequency shear elasticity of confined liquids," Proc. Natl. Acad. Sci. U. S. A. **117**(33), 19653–19655 (2020).
[21]L. Knopoff and J. N. Shapiro, "Pseudo-Grüneisen parameter for liquids," Phys. Rev. B **1**, 3893 (1970).
[22]O. L. Anderson, "The Grüneisen parameter for the last 30 years," Geophys. J. Int. **143**, 279 (2000).
[23]R. Munier, C. Doudard, S. Calloch, and B. Weber, "Determination of high cycle fatigue properties of a wide range of steelsheet grades from self-heating measurement," Int. J. Fatigue **63**, 46 (2014).
[24]M. Baggioli, M. Landry, and A. Zaccone, "Deformations, relaxation and broken symmetries in liquids, solids and glasses: A unified topological field theory," arXiv:2101.05015.
[25]L. Noirez, P. Baroni, and J. F. Bardeau, "Highlighting non-uniform temperatures close to liquid/solid surface," Appl. Phys. Lett. **110**, 213904 (2017).
[26]F. Volino, "Théorie visco-élastique non-extensive," Ann. Phys. **22**(1–2), 7–41 (1997).
[27]K. Trachenko, "Lagrangian formulation and symmetrical description of liquid dynamics," Phys. Rev. E **96**, 062134 (2017).
[28]M. Baggioli, V. Brazhkin, K. Trachenko, and M. Vasin, "Gapped momentum states," Phys. Rep. **865**, 1–44 (2020).
[29]T.-D. Li and E. Riedo, "Nonlinear viscoelastic dynamics of nanoconfined wetting liquids," Phys. Rev. Lett. **100**, 106102 (2008).